Journal of Naval Architecture and Marine Engineering
January, 2025
http://dx.doi.org/10.3329/jname.v22i1.76875 http://www.banglajol.info

HEAT AND MASS TRANSFER OF MHD WILLIAMSON FLUID FLOW PAST A SHRINKING/STRETCHING SHEET WITH DUAL STRATIFICATION, RADIATION, JOULE HEATING EFFECTS

Vardireddy Sujatha[1], Wuriti Sridhar[2*]

[1]Research Scholar, Department of Mathematics, Koneru Lakshmaiah Educational Foundation, Vaddeswaram, Guntur, 522302, A.P., India, vardireddysujatha85@gmail.com

[2*]Department of Mathematics, Koneru Lakshmaiah Educational Foundation, Vaddeswaram, Guntur, 522302, A.P., India, Email: sridharwuriti@gmail.com

Abstract:

The current study examines the Williamson fluid flow on a stretching surface under the effects of MHD and porous material. In addition, the effects of different characteristics such as heat source, viscous dissipation, joule heating effect and chemical reaction are examined. The influence of solutal stratification factors and temperature was also investigated. Partial differential equations are used to represent the problem's governing non-linear equations. After applying the required similarity transformations, these equations are transformed into a collection of non-linear ordinary differential equations. The Keller Box method is used to solve the resulting equations numerically. Plotting the velocity, temperature, and concentration graphs allows for the examination of the effects of different parameters. Additionally, local parameters are computed and compared with findings from earlier research; the results show compatibility. Profiles of velocity exhibit decreasing behaviour in case of Williamson, Magnetic, and Permeable parameter raises. Profiles of temperature exhibits the increasing tendency in case of Williamson, Magnetic, the effect of Radiation, Joule heating, Heat source and Eckert number whereas opposite trend is witnessed in case of Prandtl number, thermal stratification parameters raises. Concentration profiles enhances in case of Williamson, magnetic, permeability parameters and opposite behaviour is examined in case of chemical reaction, solutal stratification, Schmidt number parameters.

Keywords: MHD, Williamson fluid, dual stratification, radiation, Joule heating.

NOMENCLATURE ***Greek symbols***

x ,y	Cartesian coordinates	ρ	Density (kg/m^3)
u, v	Velocity components(m/s)	v	Kinematic viscosity (m^2/s)
Γ	Williamson time constant	k'	Permeability of the Porous medium(m^2)
T	Fluid temperature (^{0}C)	c_p	Specific heat at constant pressure(J·kg^{-1}·K^{-1})
T_∞	Ambient fluid temperature(^{0}C)	k_r	Reaction rate (mol·L^{-1}·s^{-1})
D	Diffusion coefficient (m^2/s)	C_0	Fluid concentration (kg/m^3)
μ	Dynamic viscosity (N. s/m^2)	C_∞	Ambient fluid concentration (kg/m^3)
k	Thermal conductivity (W/m•K)	Q	Heat absobtion/generation (kelvin)

1. Introduction

Heat transfer in non-Newtonian fluid flow through porous medium is of great practical importance in a wide range of applications, including packed bed reactors, transportation processes, the disposal of nuclear waste in the field of chemical engineering, improved methods of food preservation in the field of food technology, the exploration of geo-pressurized reservoirs and the extraction of geothermal energy in the field of geophysics, oil recovery mechanisms in the field of petroleum engineering as mentioned by Shenoy (1994). Typical micro models consisting of capillary networks applied at the sub-Darcy scale are parameterized for non-Newtonian fluid flows is discussed in their study by Pearson and Tardy (2002). Hameed and Nadeem (2007) during this study, non-Newtonian fluid flow was studied through a permeable medium, as well as the presence of material constants in second-order fluids and their influence on the velocity field. Khan and Latifizadeh (2013) studied

 Received on: Oct., 2024

MHD non-Newtonian fluid flow through elongated sheet using the new optimal homotopy perturbation scheme and ADM method.

Nadeem and Hussain (2014) examined Williamson fluid flow through a stretching surface along with the influence of nanoparticles using the HAM technique and noted an increment in temperature gradient with enhancement of Lewis number and diffusivity ratio. Zehra *et al.* (2015) examined Williamson fluid flow over an inclined channel with the impact of pressure-actuated viscosity and permeability and observed that Weissenberg numbers increase the velocity of fluid flow. Hayat *et al.* (2016) describe the impact of an electric and magnetic field on Williamson fluid flow over an unstable extended sheet, as well as temperature enhancement. Jain and Parmar (2017) invented the radiation impact of Williamson fluid flow over a stretched cylinder using the RK method and witnessed temperature distribution enhancement for growing thermal radiation parameter values. Bibi *et al.* (2018) studied time-dependent Williamson fluid stream over an absorbent elongated sheet and noticed that skin friction values increase for higher unsteadiness parameter values. When examining the impact of MHD on the oscillatory flow of Williamson fluid through a porous channel, Khudair and Khafajy (2018) discovered that the velocity profile reduces as the magnetic parameter increases. Penezai *et al.* (2019) discovered that the velocity profile of a mixed convective flow over a permeable wedge decreases as the Williamson parameter rises. Kebede *et al.* (2020) found that higher values of thermal radiation and chemical reactions result in a faster mass transfer rate in Williamson nanofluid stream's marginal layer flow across a stretched sheet. Bouslimi *et al.* (2021) observed an increase in the temperature distribution in the electromagnetic flow of a Williamson Nano fluid stream in order to obtain better values of the heat generation parameter and the Eckert number. Meenakumari *et al.* (2021) discovered that in Williamson nanofluid flows on a stretching permeable surface that is vertically orientated, the thermal boundary layer width reduced as the viscous dissipation parameter increased. Following this, Reddy *et al.* (2022) addressed the effects of slip on Williamson nanofluid flow, specifically how the temperature and concentration profile decrease as the thermal slip parameter rises. Fluid heating and cooling is essential in many industries, such as transportation and power generation. A more efficient heat transfer medium is just one additional way the base fluid can improve thermal conductivity as reported by Ullah (2022). The Sakiadas flow of Williamson fluid under the influence of joule heating, solar radiation, and varying density was numerically explored by Abbas *et al.* (2023). An increase in the verifiable density parameter for heat transfer is observed for radiation values that are on the rise. In their investigation of the effects of radiation on Williamson nanofluid flow over a thin cylinder, Zaman *et al.*(2024) found that the temperature profile exhibited both rising and falling trends for incremental measurements of the Prandtl number and radiation parameters. Sankari *et al*. (2024) research on bioconvective fluxes in Williamson nanofluid flow across an exponentially stretched sheet revealed that the activation energy drops as the chemical reaction increases.

Kumar *et al.* (2020) examined Williamson fluid flow under the effects of non-linear thermal radiation and Joule heating, they found that heat transmission decreased as the Eckert number increased. Tarakaramu *et al.* (2022) demonstrated the influence of viscous dissipation and Joule heating on Williamson Nano fluid flow over an extending surface with melting conditions concludes that Williamson Nanofluid's heat transfer rate is more efficient than nanofluid. In their study, Khan *et al.* (2023) examined the effects of radiation, porous media, and double stratification on hyperbolic tangent fluid flow. They found that velocity decreases with increasing power law index and porosity parameter values. Opposite trends are observed in case of heat and mass transfer rates for both thermal and solutal stratified parameters. Pattnaik *et al.* (2021) studied dual stratification effects on Mixed convective flow of Micropolar fluid with MHD, Radiation, viscous dissipation influence using ADM method and this study has applications in thermomagnetic coating processes involving nanomaterials. Reddy and Sridevi (2022) in their study discussed that the temperature profile deteriorates with rising observations of thermal stratification parameters. Geetha *et al.*(2022) studied double stratification effect on Williamson fluid flow over a stretching and shrinking sheet through a permeable medium with MHD, radiation impacts and concludes temperature and nusselt number reduces for enhanced values of thermal stratification parameter and also for enhanced values of solutal stratification parameter concentration profile decreases. Some researchers like Shankar *et al.* (2023), Roja et al. (2024) investigated various effects like joule heating, activation energy over different geometries. The effects of dual stratification parameters, MHD, Joule heating, viscous dissipation, and chemical reaction effects of Williamson fluid flow across a stretching/shrinking sheet were investigated in the current work. MATLAB is used to draw the graphs and the Keller box approach is used to solve the associated equations of the problem. The flow chart of the approach is shown in Figure 1(a). When the findings are compared to the body of current literature, they are discovered to be consistent with earlier research studies.

2. Formulation of the Problem

A two-dimensional Williamson fluid flow on a permeable stretching sheet is studied. Flow is considered on the stretching sheet in the direction of the x-axis. y-axis is normal to the surface as shown in Fig. 1(b). The direction of the fluid flow and the magnetic field's application are perpendicular to each other. When a fluid possesses some level of electrical conductivity, it can generate an induced magnetic field as it interacts with the applied magnetic field. However, in most cases, the strength of the induced magnetic field is likely to be weaker than that of the externally applied magnetic field

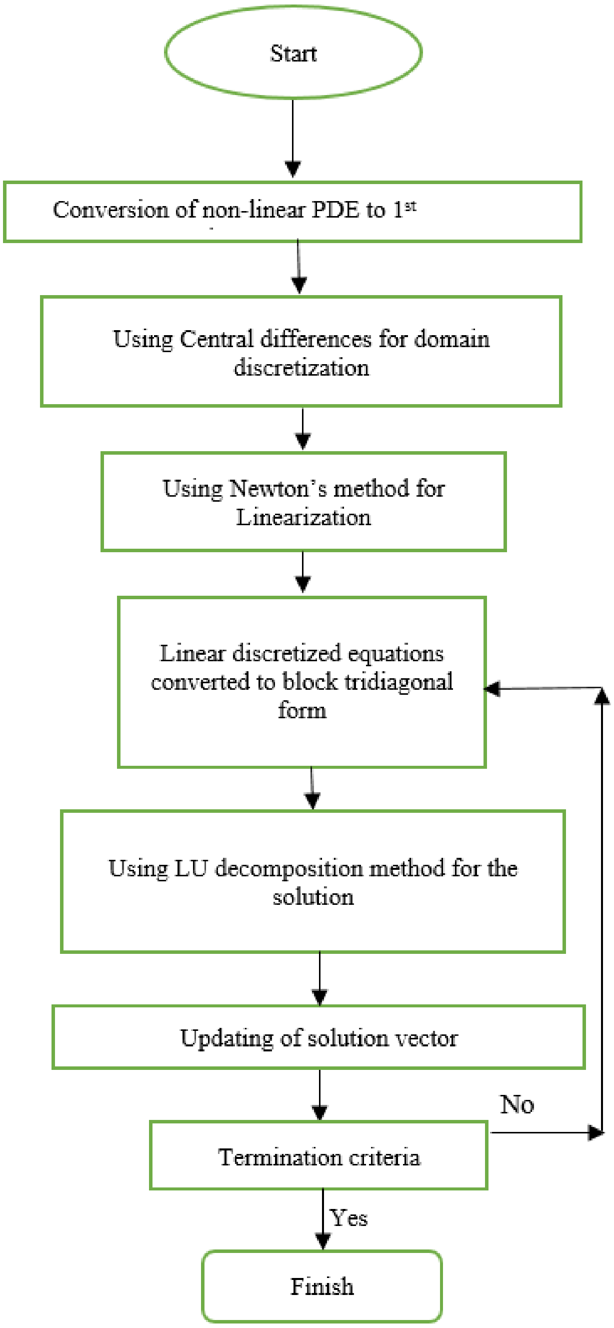

Fig. 1(a):Flowchart representation for Keller Box Scheme

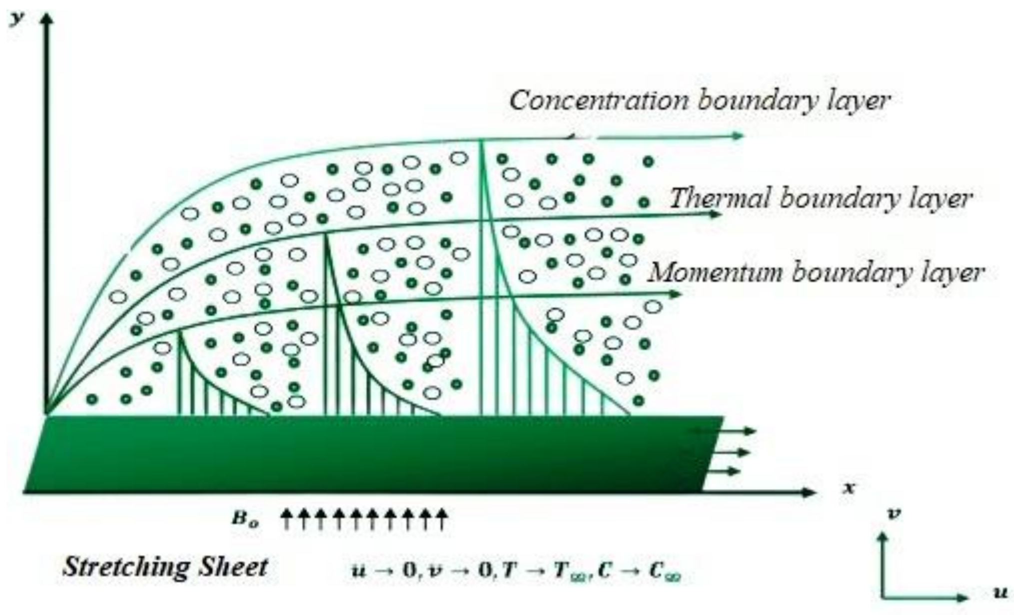

Fig. 1(b): Physical model and flow configuration

Under these assumptions the guiding partial differential equations of the problem (Geetha *et al.*,2024) are

$$\frac{\partial u}{\partial x}+\frac{\partial v}{\partial y}=0 \tag{1}$$

$$u\frac{\partial u}{\partial x}+v\frac{\partial u}{\partial y}=\upsilon\frac{\partial^2 u}{\partial y^2}+\sqrt{2}\,\upsilon\Gamma\frac{\partial u}{\partial y}\frac{\partial^2 u}{\partial y^2}-\frac{\sigma B^2}{\rho}u-\frac{\upsilon}{k'}u \tag{2}$$

$$u\frac{\partial T}{\partial x}+v\frac{\partial T}{\partial y}=\frac{k}{\rho c_p}\frac{\partial^2 T}{\partial y^2}+\frac{Q}{\rho c_p}(T-T_\infty)+\frac{\mu}{\rho c_p}\left(\frac{\partial u}{\partial y}\right)^2+\frac{\sigma B_0^2}{\rho c_p}u^2-\frac{1}{\rho c_p}\frac{\partial q_r}{\partial y} \tag{3}$$

$$u\frac{\partial C}{\partial x}+v\frac{\partial C}{\partial y}=D\frac{\partial^2 C}{\partial y^2}-k_r(C-C_\infty) \tag{4}$$

where u ,v, υ, ρ , k' ,T ,T_∞, c_p ,k_r D ,C_∞ were mentioned in nomenclature.

the corresponding boundary conditions of the problem are

$$u=U_w,\ v=-v_w,\ T=T_w=T_0+a_1x,\ C=C_w=C_0+b_1x \quad \text{at} \quad y=0$$

$$u\to 0,\ T\to T_\infty=T_0+a_2x,\ C\to C_\infty=C_0+b_2x \ \text{as}\ y\to\infty \tag{5}$$

Where, $U_w=c\,x$ for stretching sheet case and $U_w=-c\,x$ is for shrinking sheet, with $c>0$ the contraction amount or expansion held constant. v_w speed at which mass is transferring upon a wall in preparation $v_w>0$ for the mass injection $v_w<0$ orthe mass suction.

Introducing the similarity transformations as follows

$$\psi=\sqrt{c\upsilon}\,x\,f(\eta),\ \eta=y\sqrt{\frac{c}{\upsilon}} \quad T=T_\infty-\theta(\eta).(T_0-T_w),\ C=C_\infty-\phi(\eta).(C_0-C_w) \tag{6}$$

where ψ is stream function and η is similarity variable. Based on stream function we get

$$\left.\begin{aligned} u &= \frac{\partial \psi}{\partial y} = cxf\,'(\eta) \\ v &= -\frac{\partial \psi}{\partial x} = -\sqrt{cv}\, f(\eta) \\ T &= a_1 x\theta(\eta),\ T_\infty = T_0 + a_2 x \\ C &= b_1 x\theta(\eta),\ C_\infty = C_0 + b_2 x \end{aligned}\right\} \tag{7}$$

Using the above similarity transformations, the equations (2) - (4) are reduced to

$$f''' + f\ f'' + Wi.f''\ f''' - f'^2 - (M + \lambda_2)\ f' = 0 \tag{8}$$

$$(1+Rd)\theta'' + \Pr\ f\theta' - \Pr\ f'\theta - \Pr e_1\ f' + \Pr\gamma\theta + \Pr Ecf\ ''^2 + \Pr Jf\ '^2 = 0 \tag{9}$$

$$\phi'' + Sc\left(f\phi' - f'\phi - K_1\phi\right) = 0 \tag{10}$$

The applicable boundary conditions (5) are converted to

$$f = S,\ \ f' = 1,\ \ \theta = 1 - e_1,\ \ \phi = 1 - e_2 \text{ at } \ \eta = 0$$

$$f' = 0,\ \ \theta = 0,\ \ \phi = 0 \qquad \text{as} \quad \eta \to \infty \tag{11}$$

where $Wi = \Gamma x\sqrt{\dfrac{2c^3}{\upsilon}}$, $M = \dfrac{\sigma B_0^2}{\rho c}$, $\lambda_2 = \dfrac{\upsilon}{k'c}$, $\Pr = \dfrac{\mu c_p}{k}$, $e_1 = \dfrac{a_2}{a_1}$, $\gamma = \dfrac{Q}{c\rho c_p}$, $Sc = \dfrac{\upsilon}{D}$, $e_2 = \dfrac{b_2}{b_1}$

$K_1 = \dfrac{k_r}{c}$ and $S = \dfrac{v_w}{\sqrt{c\upsilon}}$ (with $S > 0$ (i.e., $v_w > 0$) wall mass suction and $S < 0$ (i.e., $v_w < 0$) wall mass injection), Ec represents Eckert number, J represents Joule heating parameter. Moreover, the drag force coefficient in terms of C_j , Nusselt and Sherwood numbers are determined by:

$$\sqrt{\mathrm{Re}_x}\, C_f = -\left(f''(0) + \frac{Wi}{2}\left(f''(0)\right)^2 \right),\quad \frac{Nu}{\sqrt{\mathrm{Re}_x}} = -\theta'(0),$$

$$\frac{Sh}{\sqrt{\mathrm{Re}_x}} = -\phi'(0), \text{where } \ \mathrm{Re}_x = \frac{U_w x}{\upsilon} \tag{13}$$

3. Methodology

Introducing $\dfrac{df}{d\eta} = p, \dfrac{dp}{d\eta} = q, \dfrac{dg}{d\eta} = t, \dfrac{ds}{d\eta} = n$ (14)

equations (8,9,10) converted to

$$q' + Wiqq' + fq - p^2 - (M + \lambda_2)p = 0 \tag{15}$$

$$(1+Rd)t' + \Pr\ ft - \Pr\ pg - \Pr e_1 p + \Pr\gamma g + \Pr Ecq^2 + \Pr Jp^2 = 0 \tag{16}$$

$$n' + Scfn - Scps - ScK_1 s = 0 \tag{17}$$

Applying Newton's technique and the idea of finite differences, the equations (14–16) are converted to a system of linear equations.

The tri-diagonal system's equations in matrix form takes the form as

$$\left.\begin{aligned} &[A_1][\delta_1] + [C_1][\delta_2] = [r_1], \\ &[B_1][\delta_1] + [A_2][\delta_2] + [C_2][\delta_3] = [r_2], \\ &\dots\dots \\ &[B_{j-1}][\delta_1] + [A_{j-1}][\delta_2] + [C_{j-1}][\delta_3] = [r_{j-1}], \\ &[B_j][\delta_{j-1}] + [A_j][\delta_j] = [r_j], \end{aligned}\right\} \tag{18}$$

along with

$$(A_1)=\begin{bmatrix} 0 & 0 & 0 & 1 & 0 & 0 & 0 \\ -\frac{h_j}{2} & 0 & 0 & 0 & -\frac{h_j}{2} & 0 & 0 \\ 0 & -\frac{h_j}{2} & 0 & 0 & 0 & -\frac{h_j}{2} & 0 \\ 0 & 0 & -1 & 0 & 0 & 0 & -\frac{h_j}{2} \\ (a_2)_1 & 0 & 0 & (a_3)_1 & (a_1)_1 & 0 & 0 \\ (b_{10})_1 & (b_2)_1 & 0 & (b_7)_1 & (b_9)_1 & (b_1)_1 & 0 \\ 0 & 0 & (c_6)_1 & (c_3)_1 & 0 & 0 & (c_1)_1 \end{bmatrix}$$

$$(A_j)=\begin{bmatrix} -\frac{h_j}{2} & 0 & 0 & 1 & 0 & 0 & 0 \\ -1 & 0 & 0 & 0 & -\frac{h_j}{2} & 0 & 0 \\ 0 & -1 & 0 & 0 & 0 & -\frac{h_j}{2} & 0 \\ 0 & 0 & -1 & 0 & 0 & 0 & -\frac{h_j}{2} \\ (a_6)_j & (a_8)_j & 0 & (a_3)_j & (a_1)_j & 0 & 0 \\ (b_6)_j & (b_4)_j & 0 & (b_7)_j & (b_9)_j & (b_1)_j & 0 \\ 0 & 0 & (c_6)_j & (c_3)_j & 0 & 0 & (c_1)_j \end{bmatrix}$$

$$(B_j)=\begin{bmatrix} 0 & 0 & 0 & -1 & 0 & 0 & 0 \\ 0 & 0 & 0 & 0 & -\frac{h_j}{2} & 0 & 0 \\ 0 & 0 & 0 & 0 & 0 & -\frac{h_j}{2} & 0 \\ 0 & 0 & 0 & 0 & 0 & 0 & -\frac{h_j}{2} \\ 0 & 0 & 0 & (a_4)_j & (a_2)_j & 0 & 0 \\ 0 & 0 & 0 & (b_8)_j & (b_{10})_j & (b_2)_j & 0 \\ 0 & 0 & (c_4)_j & 0 & 0 & 0 & (c_2)_j \end{bmatrix}$$

$$(C_j)=\begin{bmatrix} -\frac{h_j}{2} & 0 & 0 & 0 & 0 & 0 & 0 \\ 1 & 0 & 0 & 0 & 0 & 0 & 0 \\ 0 & 1 & 0 & 0 & 0 & 0 & 0 \\ 0 & 0 & 1 & 0 & 0 & 0 & 0 \\ (a_5)_j & (a_7)_j & 0 & 0 & 0 & 0 & 0 \\ (b_5)_j & (b_3)_j & 0 & 0 & 0 & 0 & 0 \\ 0 & 0 & (c_5)_j & 0 & 0 & 0 & 0 \end{bmatrix}$$

The linear system of equations is transformed in to matrix form. The result system of equations is solved using Block tri-diagonal elimination technique. The calculations continue until the desired convergence criterion is satisfied. The process stops once the value becomes sufficiently small and reaches the recommended threshold $\left|\delta g_0^{(i)}\right| < \varepsilon$.

4. Results and Discussion

To analyze the problem the graphs of velocity, temperature and concentration profiles are plotted using MATLAB.

4.1 Velocity profiles

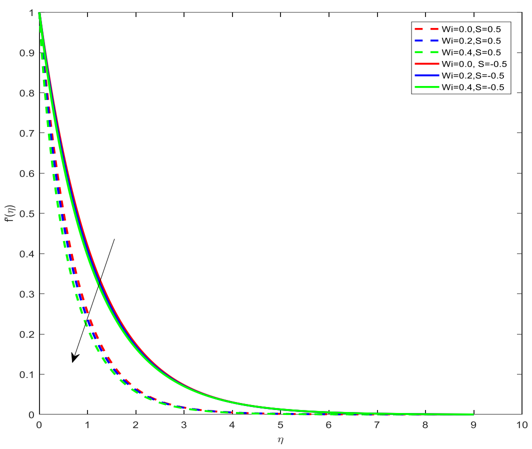

Fig. 2: Outlines of $f'(\eta)$ against Wi

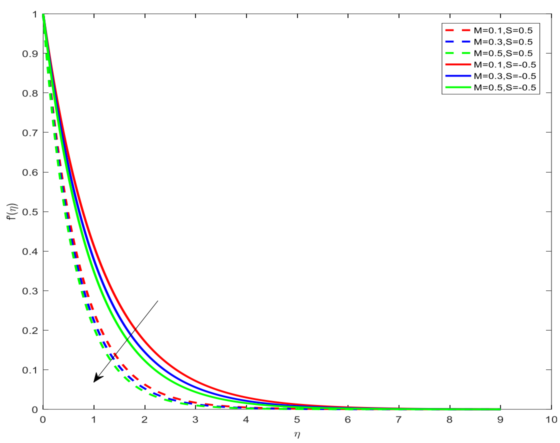

Fig. 3: Outlines of $f'(\eta)$ against M.

Figures 2-4 represent velocity profiles of Wi, M, λ_2 respectively. For increasing observations of Williamson parameter velocity profile decreases in both cases of suction/injection. On increasing Williamson parameter viscosity of the fluid increases which causes reduction in velocity profile which is depicted in Figure 2. For higher values of Magnetic parameter an opposing force which is called as the Lorentz force is generated. So velocity profile decreases portrayed in Figure 3. Enhancing porosity increases frictional force causes decrement in velocity profiles displayed in Figure 4. Nusselt number is computed for progressive values of the Prandtl number and compared with results from earlier research that are consistent with the body of literature, as shown in Table 2

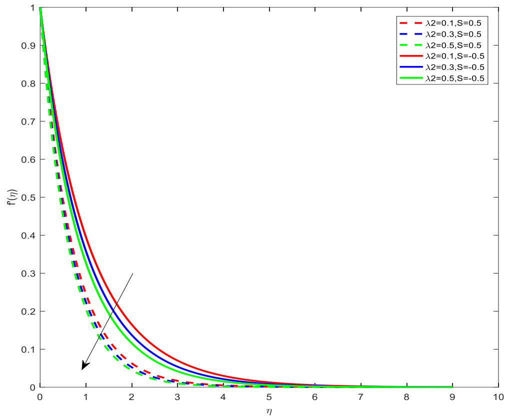

Fig. 4: Outlines of $f'(\eta)$ against λ_2

4.2 Temperature profiles

Figures 5-13 represent the temperature profiles of Wi, Pr, Rd, M, J, γ, Ec, λ_2, e_1 respectively. Increasing Williamson parameter temperature increases because of enhancement in the elasticity stress parameter as mentioned in Figure 5. The fluid's thermal conductivity decreases for improved Prandtl number observations, which results in a decline in the temperature profiles seen in Figure 6.. For greater observations of radiation parameter more heat will be produced causes enhancement in temperature distribution in both cases of suction/injection as shown in Figure 7. As the magnetic field parameter is increased, the thickness of the thermal boundary layer rises, resulting in the temperature profile rising seen in Figure 8.

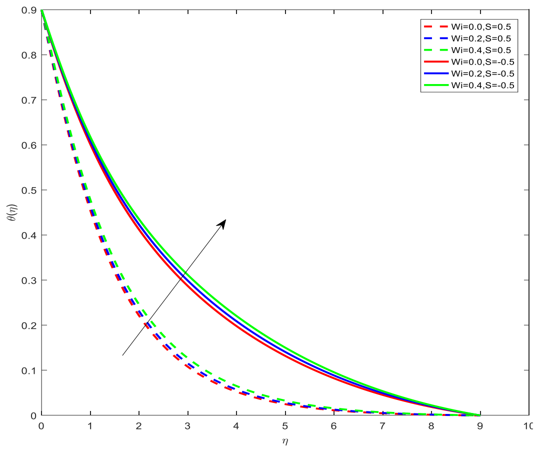

Fig. 5: Outlines of $\theta(\eta)$ against Wi

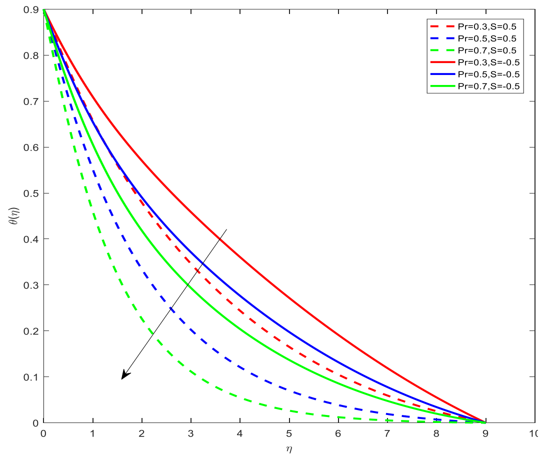

Fig. 6: Outlines of $\theta(\eta)$ against Pr

For incremental observations of Joule heating parameter causes increment in conductivity of the fluid increases so temperature enhancement is noted portrayed in Figure 9. For incremental measurements of heat source parameter temperature of the fluid raises in both cases of suction/injection mentioned in Figure 10.The fluid's kinetic energy increases with rising Eckert number, which raises the temperature as seen in Figure 11. For larger values of permeability parameter frictional force is generated inside the fluid causes augmentation in temperature profiles as displayed in Figure 12. As thermal stratification parameter increases, the temperature differential betwee Concentration profiles: n the surrounding and surface air cools, resulting in a decline in temperature profiles, as illustrated in Figure 13. In Table 1, the values of the local parameters Sherwood number, skin friction coefficient number, and Nusselt number are computed and tabulated.

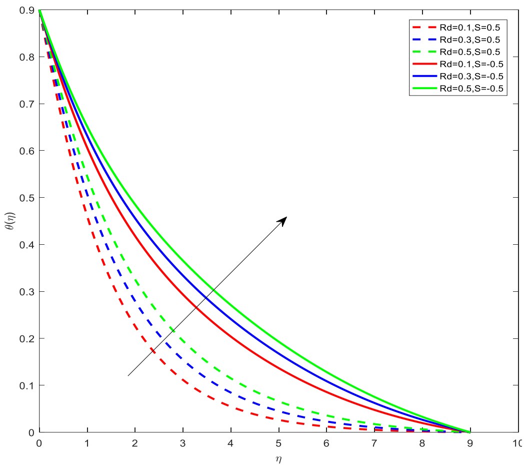

Fig. 7: Oulines of $\theta(\eta)$ against Rd

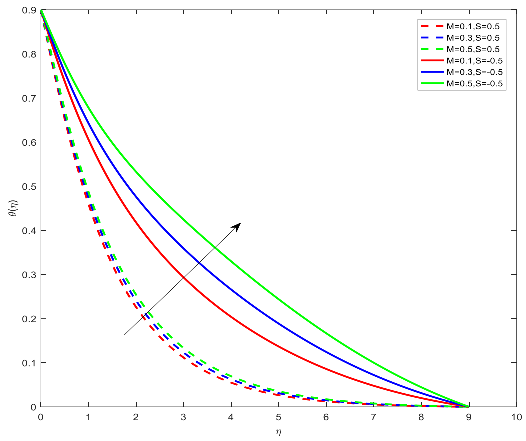

Fig. 8:Outlines of $\theta(\eta)$ against M

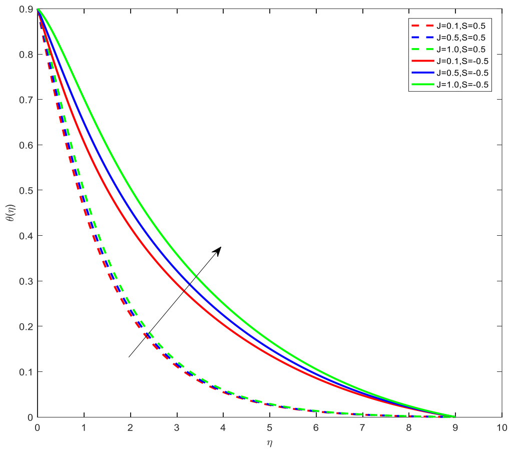

Fig. 9: Outlines of $\theta(\eta)$ against J

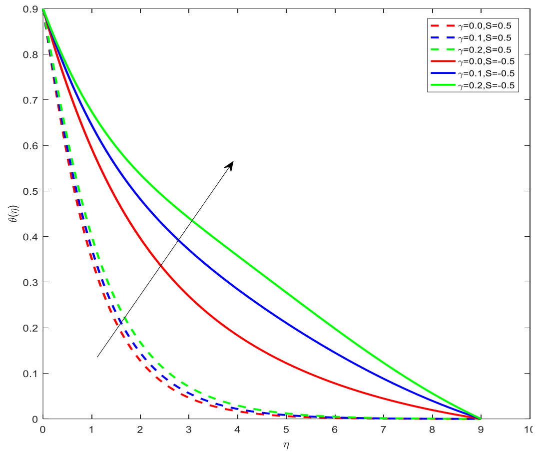

Fig. 10: Outlines of $\theta(\eta)$ against γ

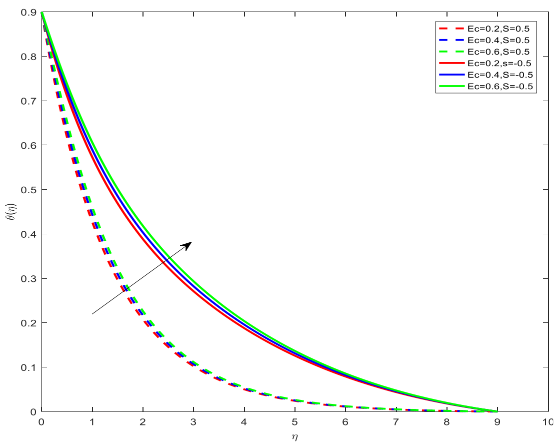

Fig. 11: Outlines of $\theta(\eta)$ against Ec

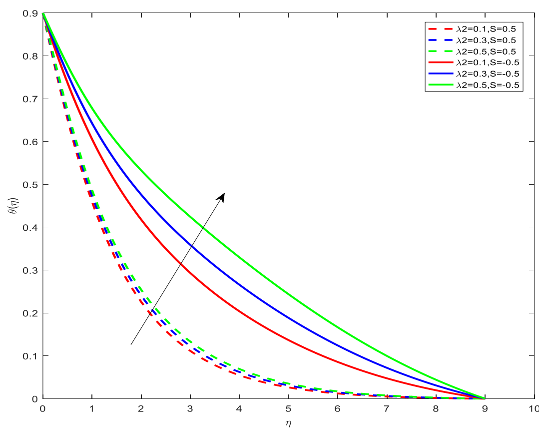

Fig. 12: Outlines of $\theta(\eta)$ against λ_2

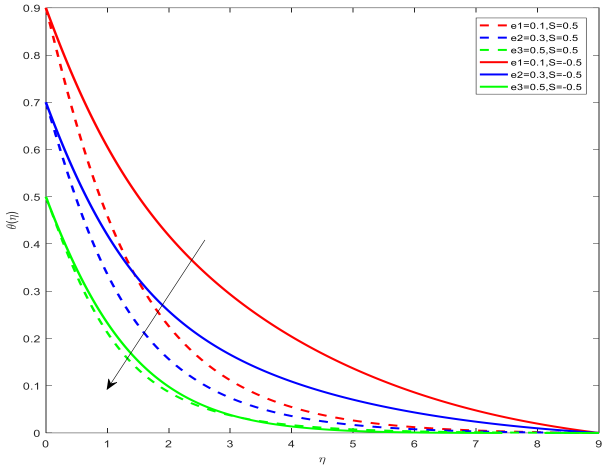

Fig.13: Outlines of $\theta(\eta)$ against e_1

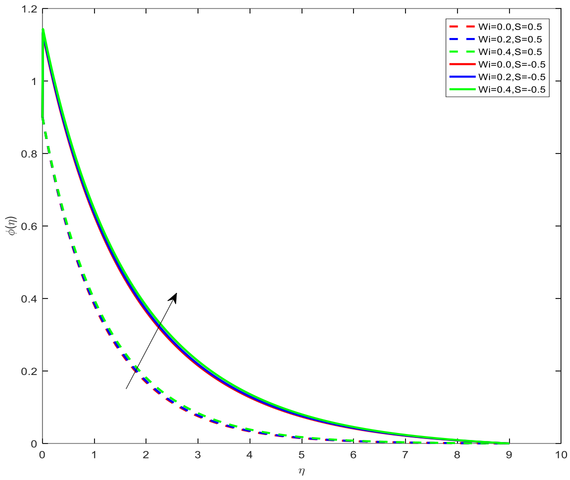

Fig. 14: Outlines of $\phi(\eta)$ against Wi

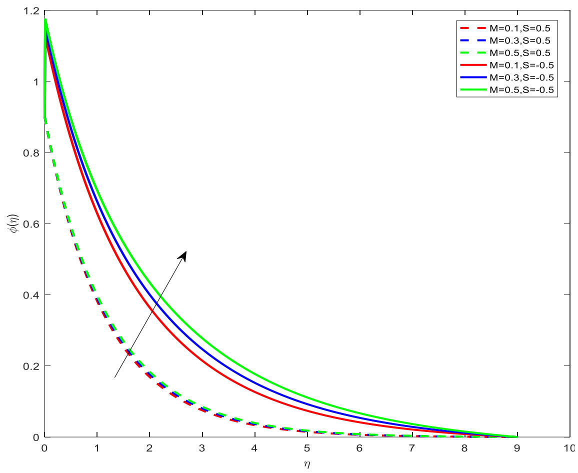

Fig. 15: Outlines of $\phi(\eta)$ against M

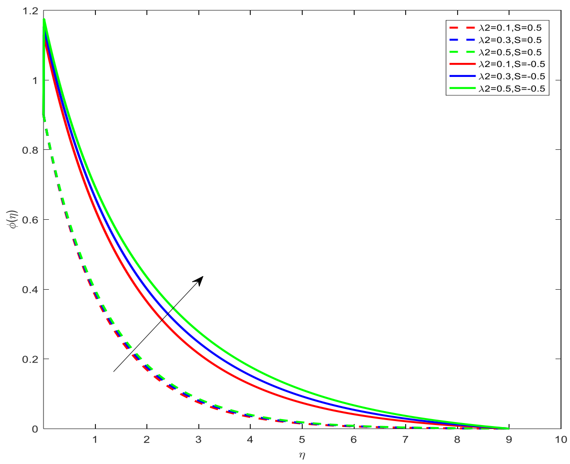

Fig. 16: Outlines of $\phi(\eta)$ against λ_2

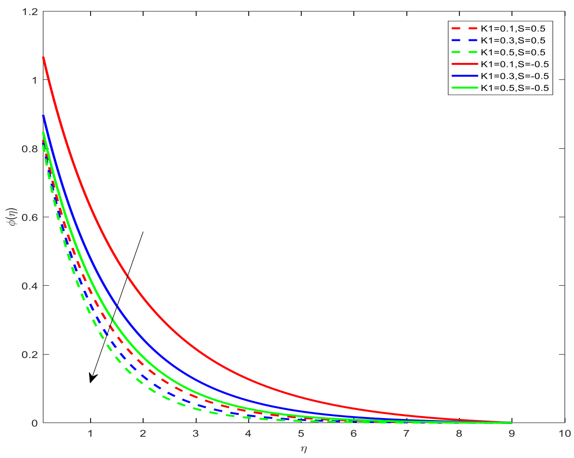

Fig. 17: Outlines of $\phi(\eta)$ against K1

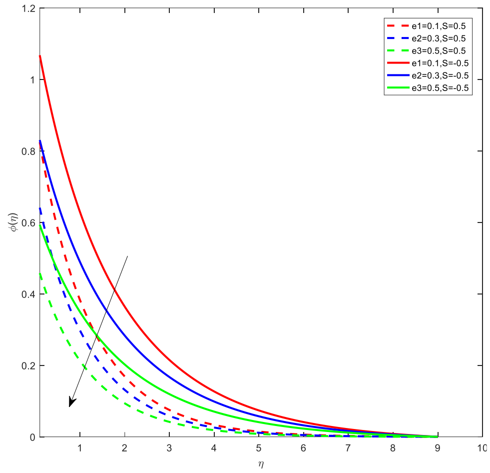

Fig. 18: Outlines of $\phi(\eta)$ against e_2

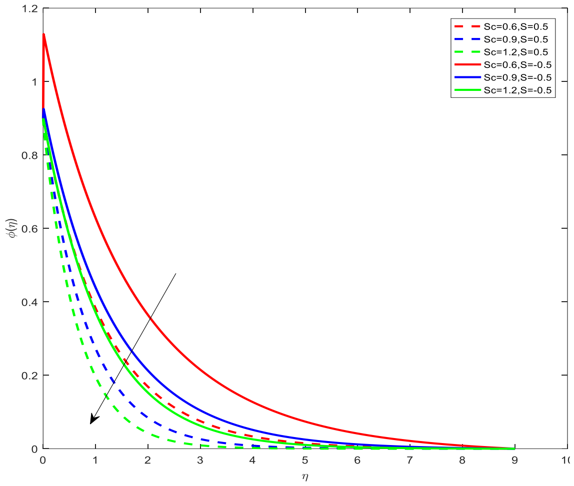

Fig. 19: Outlines of $\phi(\eta)$ against Sc

Table 1: Skin friction coefficient, Nusselt number, and Sherwood number values

Wi	M	λ_2	Pr	e_1	γ	Sc	K_1	e_2	S	Rd	Ec	J	$f''(0)$	$-\theta'(0)$	$-\phi'(0)$
0.1													-2.333	1.3236	0.6746
0.2													-2.0786	1.288	0.6684
	0.2												-2.6158	1.2982	0.669
	0.3												-2.6621	1.2931	0.6687
		0.3											-2.7086	1.288	0.6684
		0.4											-2.7556	1.2828	0.6681
			0.7										-2.7556	1.2994	0.6681
			0.9										-2.7556	1.3948	0.6681
				0.3									-2.7556	1.0841	0.6681
				0.5									-2.7556	0.7735	0.6681
					0.1								-2.7556	0.7852	0.6681
					0.3								-2.7556	0.7617	0.6681
						0.2							-2.7556	0.7617	0.5186
						0.4							-2.7556	0.7617	0.5963
							0.3						-2.7556	0.7617	5848
							0.5						-2.7556	0.7617	0.5936
								0.2					-2.7556	0.7617	1.1872
								0.4					-2.7556	0.7617	1.0388
									-1				-1.1807	0.4828	0.776
									1				-2.7556	0.7617	1.0388
										0.3			-2.7556	0.667	1.0388
										0.6			-2.7556	0.383	1.0388
											0		-2.7556	0.3668	1.0388
											0.2		-2.7556	0.3966	1.0388
												0.5	-2.7556	0.3509	1.0388
												1	-2.7556	0.2937	1.0388

4.3 Concentration profiles

Figures 14-19 represents concentration profiles of Wi, M, λ_2, K1, e_2 , Sc respectively. For enhanced observations of Williamson parameter, the concentration flow of the fluid increases in both suction/injection parameter cases as portrayed in Figure 14. For incremental values of the magnetic parameter, the fluid particles' motion exited and swiftly diffused in the boundary's surrounding layers, causing the fluid concentration to rise as seen in Figure 15. Figure 16 displays the fluid concentration rises for a greater observation of the porosity characteristic. Increasing chemical reaction parameter chemical molecular diffusivity decreases so concentration profile decreases portrayed in Figure 17. Increased Schmidt number observations cause the fluid's viscosity to rise, which lowers the fluid's concentration as seen in Figure 18. Figure 19 illustrates how improved thermal stratification parameter measurements result in a rise in the solutal boundary layer due to both constructive reaction and heat diffusion, which lowers the fluid's concentration close to the plate in comparison to the surrounding medium.

Table 2: Values of $-\theta'(0)$ for various values of Pr.

Pr	Mukhopaday *et al.*(2013)	Geetha *et al.*(2024)	Present study	error % approximations (2013)	error% approximations (2024)
1	0.9547	0.95483	0.95406	6%	8%
2	1.4714	1.47144	1.47145	8%	8%
3	1.8961	1.89623	1.89537	3%	4%

5. Conclusions

In this paper, we examined dual stratification effects along with joule heating, viscous dissipation, radiation effect and chemical reaction a two-dimensional Williamson fluid flow upon a stretching surface immersed in porous medium. The governing equations are solved using Keller Box method. The following conclusions are obtained.

- Velocity profile decreases for growing values of Williamson parameter, Magnetic parameter, Porosity parameter.
- For incremental measurements of the Williamson, Magnetic, Joule heating, Radiation, Eckert, and Porosity parameters, the fluid's temperature increases; an opposite trend is observed for the Prandtl and thermal stratification parameters.
- Concentration profile enhances for Williamson parameter, magnetic parameter, Porosity parameter whereas reverse trend is noted in case of Chemical reaction parameter, Schmidt number.
- Nusselt number decreases for increasing observations of Williamson, Magnetic, thermal stratification, radiation and Joule heating parameters.
- For increasing observations of the Williamson, Magnetic, Chemical Reaction, and Solutal Stratification parameters, the Sherwood number decreases.

References

Shenoy, A. V. (1994): Non-Newtonian fluid heat transfer in porous media, In Advances in Heat transfer Vol. 24, pp.101-190. Elsevier. https://doi.org/10.1016/S0065-2717(08)70233-8

Pearson, J. R. A., Tardy and P. M. J. (2002): Models for flow of non-Newtonian and complex fluids through porous media, Journal of Non-Newtonian Fluid Mechanics, Vol.102, No.2, pp.447-473. https://doi.org/10.1016/S0377-0257(01)00191-4

Hameed, M., and Nadeem, S. (2007): Unsteady MHD flow of a non-Newtonian fluid on a porous plate. Journal of Mathematical Analysis and Applications, Vol.325, No.1, pp.724-733. https://doi.org/10.1016/j.jmaa.2006.02.002

Khan, Y., and Latifizadeh, H. (2013): Application of new optimal homotopy perturbation and Adomian decomposition methods to the MHD non-Newtonian fluid flow over a stretching sheet, International Journal of Numerical Methods for Heat and Fluid Flow, Vol.24, No.1, pp.124-136.

https://doi.org/10.1108/HFF-01-2012-0011
Mukhopadhyay, S. (2013): MHD boundary layer 5ow and heat transfer over an exponentially stretching sheet embedded in a thermally strati_ed medium, Alexandria Engineering Journal, Vol. 52, No. 3, pp. 259–265. https://doi.org/10.1016/j.aej.2013.02.003
Nadeem, S., and Hussain, S. T. (2014): Flow and heat transfer analysis of Williamson nanofluid, Applied Nanoscience, Vol.4,pp.1005-1012. https://doi.org/10.1007/s13204-013-0282-1
Zehra, I., Yousaf, M. M., and Nadeem, S. (2015): Numerical solutions of Williamson fluid with pressure dependent viscosity, Results in Physics, Vol.5, pp.20-25. https://doi.org/10.1016/j.rinp.2014.12.002
Hayat, T., Shafiq, A., and Alsaedi, A. (2016): Hydromagnetic boundary layer flow of Williamson fluid in the presence of thermal radiation and Ohmic dissipation, Alexandria Engineering Journal, Vol.55,No.3,pp. 2229-2240. https://doi.org/10.1016/j.aej.2016.06.004
Jain, S., Parmar, A. (2018): Radiation Effect on MHD Williamson Fluid Flow over Stretching Cylinder Through Porous Medium with Heat Source. In: Singh, M., Kushvah, B., Seth, G., Prakash, J. (eds) Applications of Fluid Dynamics. Lecture Notes in Mechanical Engineering, Springer, Singapore. https://doi.org/10.1007/978-981-10-5329-0_5
Bibi, M., Malik, M. Y., and Tahir, M. (2018): Numerical study of unsteady Williamson fluid flow and heat transfer in the presence of MHD through a permeable stretching surface, The European Physical Journal Plus, Vol.133, pp.1-15. https://doi.org/10.1140/epjp/i2018-11991-2
Khudair, W. S., Al-Khafajy, D. G. S. (2018): Influence of heat transfer on MHD oscillatory flow for Williamson fluid with variable viscosity through a porous medium. Int. J. Fluid Mechanics and Thermal Sciences, Vol.4,No.1,pp. 11-17. https://doi.org/10.11648/j.ijfmts.20180401.12
Panezai, A., Rehman, A., Sheikh, N., Iqbal, S., Ahmed, I., Iqbal, M., and Zulfiqar, M. (2019): Mixed convective magnetohydrodynamic heat transfer flow of Williamson fluid over a porous wedge, American Journal of Mathematical and Computer Modelling, Vol.4,No.3, pp.66-73. https://doi.org/10.11648/j.ajmcm.20190403.13
Kebede, T., Haile, E., Awgichew, G., and Walelign, T. (2020): Heat and mass transfer in unsteady boundary layer flow of Williamson nanofluids, Journal of Applied Mathematics, Vol.2020, No.1, pp.1890972. https://doi.org/10.1155/2020/1890972
Kumar, A.,Tripathi, R., Singh, R., and Chaurasiya, V. K. (2020): Simultaneous effects of nonlinear thermal radiation and Joule heating on the flow of Williamson nanofluid with entropy generation, Physica A: Statistical Mechanics and its Applications, Vol.551, pp.123972. https://doi.org/10.1016/j.physa.2019.123972
Bouslimi, J., Omri, M., Mohamed, R. A., Mahmoud, K. H., Abo-Dahab, S. M., and Soliman, M. S. (2021): MHD Williamson nanofluid flow over a stretching sheet through a porous medium under effects of joule heating, nonlinear thermal radiation, heat generation/absorption, and chemical reaction, Advances in Mathematical Physics, Vol.2021,No.1, pp.9950993. https://doi.org/10.1155/2021/9950993
Meenakumari, R., Lakshminarayana, P., and Vajravelu, K. (2021): Unsteady MHD flow of a Williamson nanofluid on a permeable stretching surface with radiation and chemical reaction effects, The European Physical Journal Special Topics, Vol.230, pp.1355-1370. https://doi.org/10.1140/epjs/s11734-021-00039-7
Khan, M., Rasheed, A., Salahuddin, T., and Ali, S. (2021): Chemically reactive flow of hyperbolic tangent fluid flow having thermal radiation and double stratification embedded in porous medium, Ain Shams Engineering Journal, Vol.12,No.3,pp.3209-3216. https://doi.org/10.1016/j.asej.2021.02.017
Reddy, Y. D., Mebarek-Oudina, F., Goud, B. S., and Ismail, A. I.(2022): Radiation, velocity and thermal slips effect toward MHD boundary layer flow through heat and mass transport of Williamson nanofluid with porous medium, Arabian Journal for Science andEngineering,Vol.47, No.12, pp.16355-16369. https://doi.org/10.1007/s13369-022-06825-2
Ullah, I. (2022): MHD radiative flow of Williamson nanofluid along stretching sheet in a porous medium with convective boundary conditions, Proceedings of the Institution of Mechanical Engineers, Part E: Journal of Process Mechanical Engineering, Vol.236,No.3,pp.1144-1152. https://doi.org/10.1177/09544089211058093
Tarakaramu, N. (2022): Viscous dissipation and joule heating effects on 3D magnetohydrodynamics flow of Williamson nanofluid in a porous medium over a stretching surface with melting condition, ASME Open Journal of Engineering, Vol.1,No.AOJE-21-1102, pp. 011033 (7). https://doi.org/10.1115/1.4055183

Pattnaik, P. K., Bhatti, M. M., Mishra, S. R., Abbas, M. A., and Bég, O. A. (2022): Mixed convective-radiative dissipative magnetized micropolar nanofluid flow over a stretching surface in porous media with double stratification and chemical reaction effects: ADM-Padé computation, Journal of Mathematics, Vol.2022,No.1,pp.9888379. https://doi.org/10.1155/2022/9888379

Sudarsana Reddy, P., and Sreedevi, P. (2022): Impact of chemical reaction and double stratification on heat and mass transfer characteristics of nanofluid flow over porous stretching sheet with thermal radiation, International Journal of Ambient Energy, Vol.43,No.1,pp.1626-1636. https://doi.org/10.1080/01430750.2020.1712240

Abbas, A., Khan, A., Abdeljawad, T., and Aslam, M. (2023): Numerical simulation of variable density and magnetohydrodynamics effects on heat generating and dissipating Williamson Sakiadis flow in a porous space: Impact of solar radiation and Joule heating, Heliyon, Vol.9,No.11.pp.e21726. https://doi.org/10.1016/j.heliyon.2023.e21726

Kumar, P., Yadav, R. S., and Makinde, O. D. (2023): Numerical study of Williamson fluid flow and heat transfer over a permeable stretching cylinder with the effects of Joule heating and heat generation/absorption, Heat Transfer, Vol.52, No.4, pp.3372-3388. https://doi.org/10.1002/htj.22832

Shankar Goud, B., Dharmaiah, G.(2023): Role of Joule heating and activation energy on MHD heat and mass transfer flow in the presence of thermal radiation, Numerical Heat Transfer, Part B: Fundamentals, Vol.84, No.5,pp.620–641. https://doi.org/10.1080/10407790.2023.2215917

Zaman, S. U., Aslam, M. N., Riaz, M. B., Akgul, A., and Hussan, A. (2024): Williamson MHD nanofluid flow with radiation effects through slender cylinder, Results in Engineering, Vol.22, pp.101966. https://doi.org/10.1016/j.rineng.2024.101966

Sankari, M. S., Rao, M. E., Shams, Z. E., Algarni, S., Sharif, M. N., Alqahtani, T., Irshad, K. (2024): Williamson MHD nanofluid flow via a porous exponentially stretching sheet with bioconvective fluxes. Case Studies in Thermal Engineering, Vol.59, pp.104453. https://doi.org/10.1016/j.csite.2024.104453

Geetha, R.,Reddappa, B., Tarakaramu, N., Rushi Kumar, B., and Ijaz Khan, M. (2024): Effect of Double Stratification on MHD Williamson Boundary Layer Flow and Heat Transfer across a Shrinking/Stretching Sheet Immersed in a Porous Medium, International Journal of Chemical Engineering, Vol.2024, pp.1–12. https://doi.org/10.1155/2024/9983489

Roja P., Reddy T.S., Ibrahim S.M., Parvathi M., Dharmaiah G., Lorenzini G. (2024):Magnetic Field Influence on Thermophoretic Micropolar Fluid Flow over an Inclined Permeable Surface: A Numerical Study, J. Appl. Comput. Mech., Vol.10,No.2,pp.369-382. https://doi.org/10.22055/jacm.2024.44739.4265